Polymer Bulletin (2025) 82:6629–6643
https://doi.org/10.1007/s00289-025-05783-7

ORIGINAL PAPER

Antimicrobial testing of cyanoethyl cellulose membranes incorporated with *Schinus molle* (L.) leaf extract

Mona M. AbdelMohsen[1] · Hebat-Allah S. Tohamy[2] · Hossam M. El-Masry[3] · Walid E. Abd-Allah[1] · Mohamed El-Sakhawy[2]

Received: 25 August 2024 / Revised: 10 April 2025 / Accepted: 11 April 2025 /
Published online: 14 May 2025
© The Author(s) 2025

Abstract

Schinus molle (L.) is a dioecious plant currently widespread in many regions worldwide. The study evaluated the main phenolic and flavonoid constituents of the methanolic leaf extract of *Schinus molle* and its antioxidant activity using TEAC assay. Cyanoethyl cellulose membranes containing different concentrations of the extract were developed and optimized. The membranes physicochemical properties were characterized using Fourier-transform infrared spectroscopy (FT-IR), X-ray diffraction analysis (XRD), and scanning electron microscopy (SEM). The antimicrobial activity was studied against gram-positive and gram-negative bacteria and pathogenic yeast. The membranes containing 5% of the extract exhibited moderate antimicrobial activity against the gram-positive bacteria *Micrococcus luteus* and *Staphylococcus aureus* (12 and 13 mm, respectively) using agar well diffusion and excellent activity against the tested strains by shake flask method. The work is an approach to exploit the antimicrobial efficacy of extracts obtained from plant matrices in search of applied products of possible interest as biotechnology, food and/or pharmaceutical industries.

Keywords *Schinus molle* · Cyanoethyl cellulose · Membrane · Antimicrobial activity · Plant extract · Flavonoids · Phenolics

✉ Mohamed El-Sakhawy
elsakhawy@yahoo.com

[1] Chemistry of Medicinal Plants Department, National Research Centre, 33 El-Bohouth St., Former ElTahrir St., Dokki, P.O.12622, Giza, Egypt

[2] Cellulose and Paper Department, National Research Centre, 33 El-Bohouth St., Former ElTahrir St., Dokki, P.O.12622, Giza, Egypt

[3] Chemistry of Natural Microbial Products Department, National Research Centre, 33 El-Bohouth St., Former ElTahrir St., Dokki, P.O.12622, Giza, Egypt

Introduction

*Schinus molle (*L.) (*S molle*), commonly known as Peruvian pepper, is an evergreen tree belonging to the Anacardiaceae family. It has been introduced in many world countries as an ornamental plant [1]. All parts of the plant have been used in traditional medicine for treating various ailments [2–4]. Many pharmacological properties have been attributed to this pepper tree, such as antioxidant, antifungal, antiproliferative, and antimicrobial activities [5, 6]. Phytochemical studies of *S. molle* have isolated terpenes, flavonoids, alkaloids, tannins, and essential oils [7–9]. The antimicrobial properties of *S. molle* leaf compounds revealed their importance towards the effect of its extracts, thus constituting a potential pharmaceutical interest [5, 10].

Cellulose and its derivatives have gained much attention. They are used in diverse fields, including paper, drugs, food industries, and more. Cellulose-based derivatives are beneficial due to their recyclability, reproducibility, biocompatibility, biodegradability, cost-effectiveness, and wide range of applicability in several fields [11–14]. Due to its notable physicochemical characteristics, cyanoethyl cellulose (CEC) has become a subject of significant scientific interest [15]. For instance, these properties make CEC good for packaging applications. Further modification of cyanoethyl groups can give products with adsorption [16], reducing and stabilizing property [17].

From the perspective of enhancing the studies that have been carried out to benefit from the antimicrobial activity of extracts obtained from plant matrices and in search for new products of possible interest application, this work aimed to study the antimicrobial efficiency of CEC membranes incorporated with *S. molle* leaf extract which was previously proven to possess antimicrobial potential [5, 10]. The extract was analysed for total phenolic and total flavonoid contents, antioxidant activity and RP-HPLC quantification of primary phenolic acids and flavonoids. The physicochemical properties of the extract-incorporated membranes were characterized using Fourier Transform Infrared (FTIR) spectroscopy, X-ray diffraction analysis (XRD), and Scanning Electron Microscopy (SEM). The reflected work is a vital approach in the conversion of organic matter to value-added product. Consequently, the processed biopolymer films showed valid potential as green bioactive alternatives for various applications.

Materials and methods

Chemicals

Reagents for spectrophotometric determination of phenolic compounds, Folin-Ciocalteu's reagent, Standards of flavonoids and phenolic compounds, and sodium carbonate were obtained from Sigma Co (St. Louis, MO, USA). For antioxidant activity, ABTS radical, Trolox and potassium persulfate; and hydroxyethyl

cellulose (HEC) and acrylonitrile (AN) were purchased from Sigma-Aldrich (Chemie GmbH, Germany). Regarding chromatographic analysis; acetonitrile, methanol and *n*-hexane were obtained from Merck (Darmstadt, Germany). All reagents used were either analytical or HPLC grade, double distilled water was used.

Plant material and extraction

Leaves of *S. molle* were collected during June and July from trees at the authorized botanical garden of Giza, Egypt, following the national institutional guidelines and regulations. A voucher specimen was identified and deposited in the herbarium of the National Research Centre.

The leaves were washed several times with tap water and then dried in an oven at 40 °C. The dried leaves were crushed into powder (500 g), extracted by maceration (3×2L) in aqueous methanol (90%), at room temperature. The methanol extract was concentrated under reduced pressure using a rotary evaporator to give a crude extract (12% w/w, 60 g).

Determination of total phenolic and flavonoid contents

The extract's total phenolic content (TPC) was estimated colorimetrically using the Folin-Ciocalteu's method. Absorbance was measured at 760 nm, and the TPC was expressed as gallic acid equivalent (mg GAE/g DW). The gallic acid calibration curve was established from 50 to 250 mg/L. Total flavonoid content (TFC) was quantified spectrophotometrically using $AlCl_3$ at 430 nm and expressed as quercetin equivalent (mg QE/g DW) [18].

Quantification of total antioxidant activity (ABTS assay)

Trolox equivalent antioxidant capacity (TEAC) was determined for the alcoholic extract of leaves as previously described (Miller & Rice-Evans, 1996). Briefly, 5 ml of 7 mM 2,2′-azinobis(3-ethyl-benzothiazoline-6-sulfonate) (ABTS) was reacted with 88 µl of 140 mM potassium persulfate solution, left 24 h in the dark to generate $ABTS^{\cdot+}$ radical cation. Before use, this solution was diluted with ethanol to give an absorbance of 0.7 ± 0.05 at 734 nm. 1 ml of the reaction mixture comprised 950 µl of $ABTS^{\cdot+}$ solution and 50 µl of the alcoholic extract was homogenized, and the absorbance measured after at least 6 min. A standard curve was obtained using different concentrations of Trolox (150–1000 mM). TEAC value was expressed as µM Trolox equivalent per g dry extract [19, 20].

HPLC analysis of phenolic and flavonoid compounds

Quantitative determination of major flavonoid and phenolic compounds was performed using HPLC apparatus, Agilent series 1200 (Agilent, USA). The apparatus equipped with autosampler injector, solvent degasser, quaternary HP pump. The diode array

(DAD) UV detector was set at 280 nm for phenolic acids and 320 nm for flavonoids. Analysis was achieved with Eclipse DB C-18 column (5 µm, 250×4.6 mm i.d.); temperature was maintained at 35 °C. Separation was done using acidified water and acetonitrile (90:10 v/v); isocratic elution at a flow rate of 1 ml/min. The injection volume for all samples was 20 µl. Standard flavonoids and phenolic acids were prepared as 10 mg/50 ml solutions in methanol and serial dilutions were done and injected into HPLC to establish standard calibration curves. Quantification of compounds was performed based on peak area computation (external standard method). The analysis was run in triplicates and the concentrations of the identified compounds were expressed as µg/g dry weight [19].

Preparation of cyanoethyl cellulose

5 g of sodium hydroxide was dissolved in 5 mL of distilled water and added to 95 mL of absolute ethyl alcohol. The alcoholic sodium hydroxide solution was introduced into a 250-mL stoppered flask equipped with a mechanical stirrer. To this, 10 g of HEC and 90 ml AN were successively added. The reaction was allowed to proceed for 2 h at room temperature. The product was filtered and washed with absolute ethyl alcohol and dried [14].

Preparation of CEC membranes

1 g of CEC was dissolved in 25 ml ethanol via homogenizer. After complete dissolution, different ratios, i.e., 2.5, 5, and 10% of the extract, were added separately to prepare CEC_1, CEC_2, and CEC_3 membranes, respectively. A blank film (without any extract) denoted as CEC film was used as a reference.

Characterization and analysis

Fourier-transform infrared spectroscopy (FT-IR)

Fourier-transform infrared spectra were collected using the KBr disk method on a Mattson 5000 spectrometer (Unicam, United Kingdom).

XRD analysis

The crystallinity was studied on X-ray powder diffraction as the diffraction patterns were measured by Bruker D-8 Advance X-ray diffractometer (Germany) applying a 40 kV voltage and a 40 mA current employing copper (Kα) radiation (1.5406 Å). The *d*-spacing (thickness), the crystallite size, dislocation density, and micro stain can be calculated by:

$$\text{Thickness}(d, nm) = \frac{\lambda}{2\sin\theta} \tag{1}$$

where θ = Bragg's angle in radians, λ = X-ray wavelength (0.1542 nm), and β & θ are full widths at half maxima and Bragg's angle of the XRD peak, respectively [12, 21].

The degree of substitution (DS) of the prepared CEC was calculated as follows [22]:

$$DS = \frac{162 \times N(\%)}{1400 - 53 \times N(\%)} \quad (2)$$

where N (%) is the nitrogen content.

SEM analysis

The morphology of samples was performed by using scanning electron microscopy (SEM, Quanta-250).

Antimicrobial activity

The antimicrobial activity of the membranes (CEC, CEC_1, CEC_2, and CEC_3) was tested by two methods; agar well diffusion and shake flask using nutrient agar plates and nutrient broth medium in 100 ml sterile conical flasks, according to El-Sakhawy et al. [11]. The selected pathogenic microorganisms used in this study included inoculations of the gram-positive bacteria *Micrococcus luteus* (ATCC10240) and *Staphylococcus aureus* (ATCC6538), the gram-negative bacteria *Escherichia coli* (ATCC25922), and the pathogenic yeast *Candida albicans* (ATCC10231). These tested organisms were made in a nutrient broth medium and incubated overnight at 37 °C. The inoculum size of the strain was designed and adjusted to approximately 0.5 McFarland standards (1.5×10^8 CFU /ml). For the agar well diffusion method, 25 µL inoculum size of each microorganism strain was spread uniformly over each plate comprising 20 ml sterile nutrient agar which was allowed to solidify. Disks of 1 cm^2 of membrane samples (CEC, CEC_1, CEC_2, and CEC_3) were arranged on the surface of the seeded plates. After placing these plates in the refrigerator for an hour for more diffusion of the samples, the plates were incubated at 35 ± 2 °C for 24 h, and the inhibition zone diameters around the membranes were observed and measured in mm [23]. For the shake flask method (diffusion in liquid medium), to calculate the (%) reduction of colony forming unit (CFU) of the tested strains, 25 µL of each of bacterial and fungal suspensions were inoculated separately to 100 ml conical flask full of sterile nutrient broth medium, supplemented with a cut of 1 cm^2 of the membranes, and then incubated, while shaking at 150 rpm at 35 ± 2 °C for 24 h. The antimicrobial potential of the membranes was evaluated by measuring the optical density every 2 h at a wavelength of 600 nm. Calculation of the (CFU %) was detected for the tested strains after treatment with the membranes, with comparison to the cells of the microorganisms that survive in the control flask after the incubation period for the bacteria and pathogenic yeast; the reduction growth rate *R* (%) for the pathogenic strains present in the flasks which were treated in relation to the control (untreated) was measured. The entire experiment was performed

in triplicate and the average values were used. The results obtained were expressed according to the following equation by [24]:

$$\text{Relative [CFU Reduction (\%)]} = (A - B/A) \times 100$$

Notice that:-
A: the CFU of pathogenic strain only in the control flask without any treatment.
B: the CFU of pathogenic strain in tested flasks after applying the treating sample.

Results and discussion

The nitrogen contents (N%) were measured with an elemental analyser and the calculated DS of the prepared CEC were 9.24% and 1.64, respectively.

TPC, TFC, and total antioxidant activity determination

TPC of leaves extract of *S. molle* was estimated as 35.22 ± 2.65 mg gallic acid equivalent (mg GAE/g D.W.) and the TFC was 16.18 ± 0.28 mg quercetin equivalent (mg QE/g D.W.). Note that the presence of different antioxidant components in the plant tissues requires several intermediate extractions to ensure maximum extraction of the available antioxidants, and since TEAC value is a quantification of the effective antioxidant activity of an extract, a higher TEAC would imply more significant antioxidant activity of the extracts [25]. Our results showed the TEAC value of the leaves extract is potentially high as 109.00 ± 6.2 µM Trolox equivalent /g extract, which is expected due to the presence of different classes of phenolic compounds.

HPLC analysis of phenolic and flavonoid compounds

Major flavonoid and phenolic compounds were quantified using the available standards (Tables 1, 2).

It showed that the main flavonoids were rutin (1870.97 µg/g) and quercetin (488.85 µg/g), along with luteolin and apigenin glycosides, and this goes along with previous results, which revealed the presence of a high content of rutin (quercetin derivative) upon the spectroscopic analysis of methanolic extract of *S. molle* [7]. In contrast, catechol (610.05 µg/g) represents the main phenolic compound in addition to caffeic (215.29 µg/g), gallic (107.66 µg/g) and *p*-coumaric (80.79 µg/g) acids, and this following the studies carried by Fedel-Miyasato et al. on the genus [26]. It worth to note that epicatechin (63.69 µg/g) is not a main phenolic compound here.

Fourier-transform infrared spectroscopy (FT-IR)

The CEC, CEC_1, CEC_2 and CEC_3 showed peaks between 3411 and 3419 (O–H), 3216–3249 (N–H), 2973–2974 (C–H), 2869–2871 (nitrile group; C≡N),

Table 1 Flavonoids identified in leaves extract of S.molle using HPLC

No	R_t	Flavonoid	Concentration (µg/g dry weight)
1	9.35	Luteolin 6-arabinose 8-glucose	67.21
2	10.53	Luteolin 6-glucose 8-arabinose	41.57
3	11.87	Apigenin 6-glucose 8-glucose	77.75
4	12.06	Luteolin 7-glucose	81.88
5	12.33	Rutin	1870.97
6	13.13	Apigenin 7-glucose	10.35
7	13.27	Quercitrin	11.73
8	14.79	Quercetin	488.85
9	14.98	Naringin	69.07
10	15.35	Hesperetin	28.8
11	16.10	Kaempferol	93.46
12	16.36	Apigenin	20.35
13	18.59	Acacetin	22.19

R_t, retention time (min)

Table 2 Phenolic compounds identified in leaves extract of *S. molle*using HPLC

No	R_t	Phenolic compound	Concentration (µg/g dry weight)
1	7.23	Gallic acid	107.66
2	8.55	Protocatechuic acid	35.59
3	8.66	Catechin	14.63
4	9.22	Chlorogenic acid	43.61
5	9.46	Catechol	610.05
6	9.61	Epicatechin	63.69
7	10.19	Caffeic acid	215.29
8	10.36	Vanillic acid	69.13
9	11.61	*P*-Coumaric acid	80.79
10	11.94	Ferulic acid	4.28
11	13.08	Ellagic acid	13.71
12	13.47	Benzoic acid	25.29
13	13.99	3,4,5-methoxy cinnamic acid	2.32
14	14.05	Coumarin	1.39
15	14.39	Salicylic acid	15.97
16	15.25	Cinnamic acid	1.12

R_t, retention time (min)

1658–1666 & 1560–1564 (anti-symmetric and symmetric stretching vibrations of C = O; as a result of the hydrolysis of acrylonitrile due to long reaction time in the preparation process of the CEC), 1404–1407 (C = C), 1373–1375 (C–O = C), 1311–1312 (C–N), 1050–1058 (C–O–C of pyranose ring and ether group) and 858–919 cm^{-1} (C–O), Fig. 1 [22, 27]. For CEC_1, CEC_2 and CEC_3, the OH

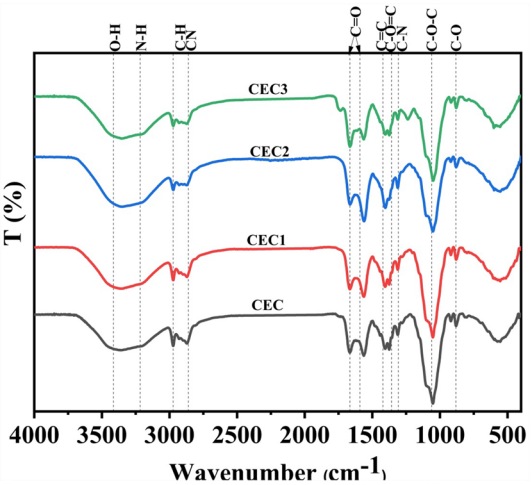


Fig. 1 FTIR spectra of blank CEC film, CEC_1, CEC_2 and CEC_3

stretching vibration of the neat CEC (3419 cm^{-1}) was moved to a lower frequency at 3411, 3405 and 3400 cm^{-1}, respectively. Creating an H–bond between the CEC and the *Schinus* extract could cause a change in the absorbance value of the OH stretching vibration [12, 13]. The O–H intensity is increased and the H–bonds among became stronger due to the substitution of O–H groups by *S molle* extract (this is proved also by MHBS calculations). In addition, LOI increased for CEC_3 compared to blank CEC membrane due to increased crystallinity (Table 3).

XRD analysis

The HEC diffractogram (Fig. 2) presented two characteristic peaks at 2θ ~ 11.78 and 21.46° which are assigned to (001) and (002) planes (i.e. amorphous and crystalline regions), respectively [12, 27]. The peak at 21.46° became broader for CEC powder compared to HEC, indicating cyanethylation occurred on the crystalline region. The CEC powder Cr.I. (%) is decreased, compared with that of HEC (Table 4), because of the cyanoethylation, which cleaved H–bonds.

Table 3 MHBS and LOI of blank CEC membrane, CEC_1, CEC_2 and CEC_3

Sample	MHBS (A_{OH}/A_{CH})	LOI (A_{1425}/A_{900})
CEC	0.96	0.84
CEC_1	0.94	0.87
CEC_2	0.96	0.86
CEC_3	0.97	0.92

MHBS, mean hydrogen bond strength; LOI, means crystallinity index

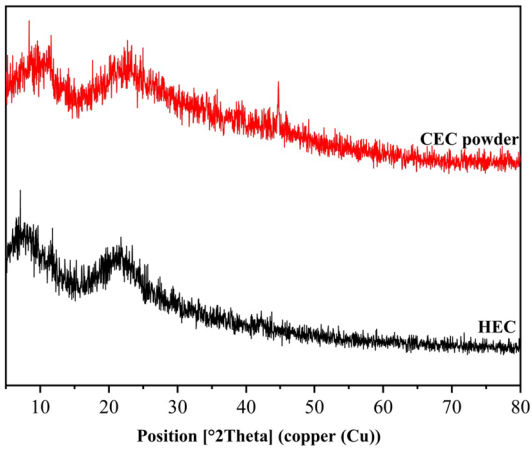


Fig. 2 XRD of HEC and CEC powder

Table 4 Crystallinity index of HEC and CEC powder

Sample	Cr.I. (%)
HEC	47.56
CEC powder	34.78

SEM analysis

Figure 3 shows the SEM images of CEC and CEC_3 films. It is clearly found that CEC and CEC_3 presented porous surface morphology with average pore sizes of ≈ 733.90 and 1146.66 nm, respectively, which indicates the effect of *S molle* extract on the CEC membrane structure (Table 5). Porosity percentage refers to the total volume of empty spaces within a material compared to its entire volume, expressed as a percentage. It does not directly tell you the number of pores or their width, CEC3 contain large pores so its porosity is high.

Antimicrobial activity

In the well diffusion method, the zone of inhibition is related to the diffusion of an antimicrobial factor in the medium after 24 h of evaluation which subsequently leads to the absence of growth of the microorganism (clear zone). The study showed that CEC_2 showed moderate antimicrobial activity against the gram-positive bacteria *Micrococcus luteus* and *Staphylococcus aureus* (12 and 13 mm, respectively) compared to the Gentamicin 10 mcg (standard antibiotic disc). The effect of the membranes on these bacteria is due to the presence of phenolic compounds; rutin, luteolin and catechol, which enters inside the bacterial cell and ceases many modes of action through inhibition of nucleic acid synthesis, followed by the inhibition of all metabolism activities and blocking biochemical reactions. These compounds'

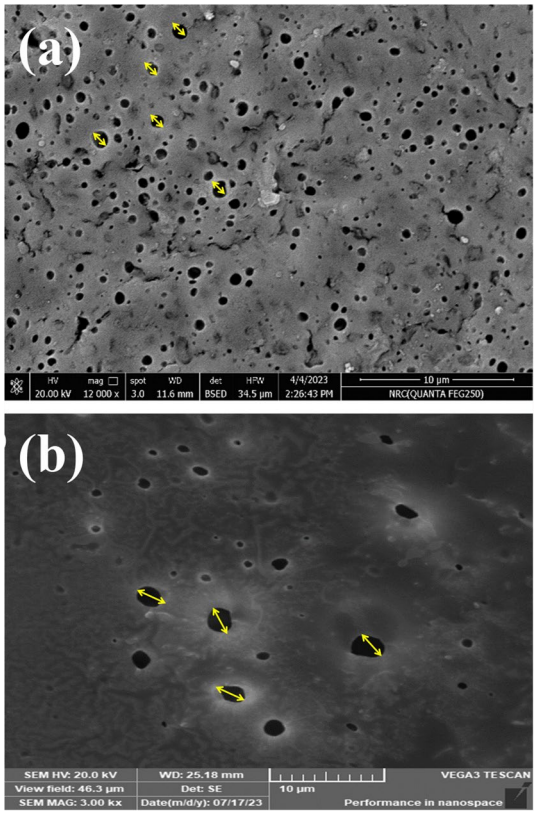


Fig. 3 SEM images of **a** Blank CEC film and **b** CEC_3

Table 5 Pore size (nm) of CEC and CEC3

Sample	Pore size (nm)
CEC	733.90
CEC3	1146.66

antimicrobial activities are well-documented and supported contribute to the antimicrobial activity together with other classes of phytocomponents present in the extract, through synergistic effect, due to the entity of polar groups which increase reactivity of the films [5, 28, 29]. Rutin demonstrates antimicrobial effects by disrupting microbial cell membranes, inhibiting enzyme activity, and interfering with microbial DNA and RNA. It also exhibits antioxidant properties, which can indirectly enhance its antimicrobial efficacy by reducing oxidative stress in host tissues. Catechol-containing compounds act by disrupting microbial cell membranes and interfering with metabolic pathways. Quercetin exhibits antimicrobial properties by disrupting microbial cell membranes, inhibiting enzyme activity, and interfering with microbial DNA replication [30–32]. The resistance of the Gram-negative bacteria could be attributed to its cell wall structure which have an effective permeability

Table 6 Inhibition zone diameter (mm) of the membranes

Tested pathogens Membranes	*Micrococcus luteus*	*Staphylococcus aureus*	*Escherichia coli*	*Candida albicans*
CEC	Nil	Nil	Nil	Nil
CEC_1	Nil	Nil	Nil	Nil
CEC_2	12.00	13.00	Nil	Nil
CEC_3	Nil	Nil	Nil	17.00
CN	28.00	26.00	21.00	Nil

Nil; no antimicrobial activity, CN; Gentamicin 10 mcg (standard antibiotic disc)

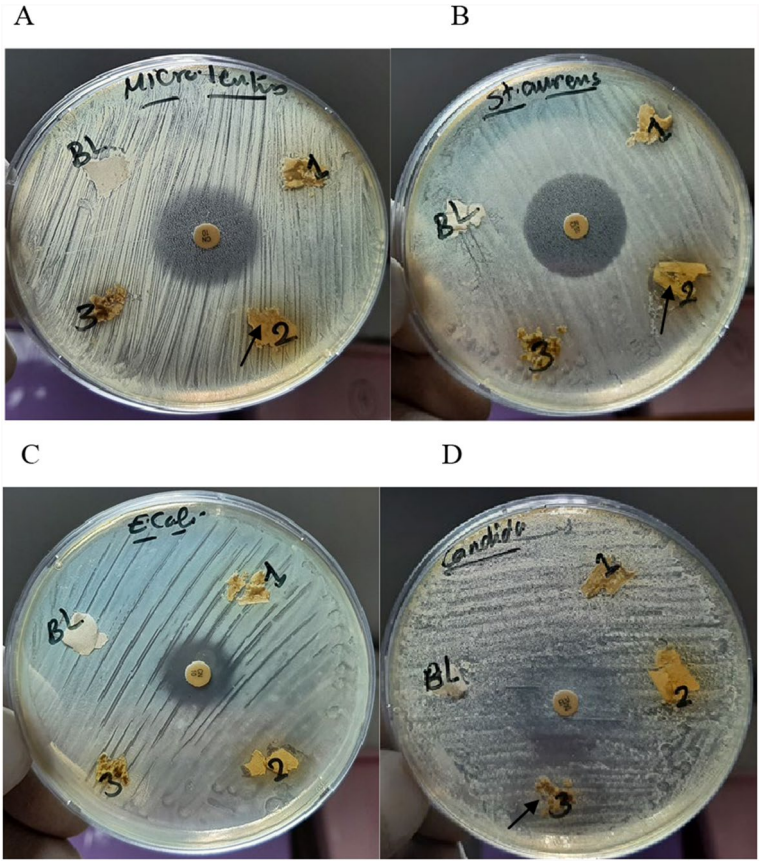


Fig. 4 Inhibition zone diameter (mm) of the tested membranes towards *Micrococcus luteus* (**A**), *Staphylococcus aureus* (**B**), *Escherichia coli* (**C**) and *Candida albicans* (**D**)

barrier comprised of a thin lipopolysaccharide exterior membrane, thus restrict the penetration of the extruding plant extract [33]. In comparison, CEC_3 showed antimicrobial activity against the pathogenic yeast *Candida albicans* (17 mm) as shown in

Table 6 and Fig. 4. This may be attributed to the higher concentration of the polyphenolic constituents [5]. Applying the shake flask method to estimate (%) reduction of colony forming unit (CFU) of the investigated organisms, more detailed information on antimicrobial kinetics was obtained.

The membranes exhibited varying degrees of activity against all microorganisms tested, as shown in Table 7. The CEC_2 showed high efficacy against all the tested organisms, comparable to that for CEC_3, and this may be due to the loaded coherence of the phenolic groups on the membrane leading to satisfactory implementation [34, 35].

By calculating the mean reduction in CFU, it showed that CEC_2 is the most effective against all pathogens. While, on calculating the weighted mean of the CFU reduction, by assigning the weight to *Candida albicans* twice the other pathogens, the results showed the significant performance of CEC_3 when dealing with *Candida albicans.* The results confirm that this pathogen was sensitive to higher concentration of the effective compounds (Table 7).

HPLC analysis of the methanolic extract of *S. molle* revealed rutin as the main component, with apigenin and other flavonoids which exert potent antimicrobial activity through membrane interference and thus lead to nucleic acid leakage [36]. Polyphenols, including catechol, which is a primary constituent in the methanolic extract, induce antimicrobial activity through irreversible changes in membrane properties, thus inducing local damage or pore formation in the cell membranes, subsequently leading to leakage of the intracellular material [37, 38].

Conclusion

Leaf extract of *S. molle* comprising compounds of bioactive molecules showed significant antioxidant and antimicrobial properties. Cyanoethyl cellulose was blended with the leaves extract in various concentrations to obtain CEC membranes suggesting their potential use in biotechnology, food and/or pharmaceutical industries. FTIR spectra showed peaks belonging to C≡N, N–H, and C–N groups as proof for cyanoethylation. SEM analysis showed the effect of *S. molle* extract on the porosity of CEC (i.e., pore size was increased after adding of the *S. molle* extract from 733.9 to 1146.6 nm). The antimicrobial activity by CFU method proved the effectiveness

Table 7 (%) reduction of colony forming unit (CFU) of the investigated organisms using shake flask method

Tested pathogens Membranes	*Micrococcus luteus*	*Staphylococcus aureus*	*Escherichia coli*	*Candida albicans*	Mean of reduction in CFU	Weighted mean of CFU reduction
MCEC	41.02	44.54	35.96	39.14	40.16	39.96
CEC_1	63.94	88.40	72.33	69.01	73.42	72.53
CEC_2	96.12	97.25	89.95	80.54	90.96	88.88
CEC_3	92.23	90.48	73.10	96.97	88.19	89.95

antimicrobial properties of the membranes. The results of the physical characterization of the films indicate their efficient utilization for diverse targets.

Acknowledgements The authors appreciate the National Research Centre, Egypt, for supporting this work.

Author contributions MMA was involved in conceptualization, supervision, investigation, writing–original draft. HST was involved in data curation, conducted the lab work, conceptualization, data analysis, investigation, writing–original draft. HME was involved in data curation, investigation, conducted the lab work, writing–original draft. WEA was involved in investigation, visualization, conducted the lab work. ME was involved in supervision, investigation, writing–review& editing. All authors read, reviewed and approved the final submitted manuscript.

Funding Open access funding provided by The Science, Technology & Innovation Funding Authority (STDF) in cooperation with The Egyptian Knowledge Bank (EKB). Not applicable.

Data availability All data generated or analysed during this study are included in this published article.

Declarations

Conflict of interest The authors have no relevant financial or non-financial interests to disclose.

Ethics approval Not applicable.

Consent to participate/consent to publish Not applicable.

Open Access This article is licensed under a Creative Commons Attribution 4.0 International License, which permits use, sharing, adaptation, distribution and reproduction in any medium or format, as long as you give appropriate credit to the original author(s) and the source, provide a link to the Creative Commons licence, and indicate if changes were made. The images or other third party material in this article are included in the article's Creative Commons licence, unless indicated otherwise in a credit line to the material. If material is not included in the article's Creative Commons licence and your intended use is not permitted by statutory regulation or exceeds the permitted use, you will need to obtain permission directly from the copyright holder. To view a copy of this licence, visit http://creativecommons.org/licenses/by/4.0/.

References

1. Taylor L (2005) The healing power of rainforest herbs: a guide to understanding and using herbal medicinals. Square One Publishers
2. Bello R et al (1998) In vitro pharmacological evaluation of the dichloromethanol extract from *Schinus molle* l. Phytother Res Int J Devoted Pharmacol Toxicol Eval Nat Product Deriv 12(7):523–525
3. Deveci O et al (2010) Chemical composition, repellent and antimicrobial activity of *Schinus molle* L. J Med Plants Res 4(21):2211–2216
4. Molina-Salinas G et al (2007) Evaluation of the flora of Northern Mexico for in vitro antimicrobial and antituberculosis activity. J Ethnopharmacol 109(3):435–441
5. Turchetti G et al (2020) Antimicrobial testing of *Schinus molle* (L.) leaf extracts and fractions followed by GC-MS investigation of biological active fractions. Molecules 25(8):1977
6. Garzoli S et al (2019) Chemical investigation of a biologically active *Schinus molle* L. leaf extract. J Anal Methods Chem 2019:8391263

7. Machado DG et al (2008) Antidepressant-like effect of rutin isolated from the ethanolic extract from *Schinus molle* L. in mice: evidence for the involvement of the serotonergic and noradrenergic systems. Eur J Pharmacol 587(1–3):163–168
8. Marzouk MS et al (2006) Antioxidant flavonol glycosides from *Schinus molle*. Phytother Res Int J Devoted Pharmacol Toxicol Eval Nat Product Deriv 20(3):200–205
9. Bendaoud H et al (2010) Chemical composition and anticancer and antioxidant activities of *Schinus molle* L. and *Schinus terebinthifolius* Raddi berries essential oils. J Food Sci 75(6):C466–C472
10. Abd-Allah WE, Awad HM, AbdelMohsen MM (2015) HPLC analysis of quercetin and antimicrobial activity of comparative methanol extracts of Shinus molle L. Int J Curr Microbiol App Sci 4(11):550–558
11. El-Sakhawy M et al (2024) Biodegradable carboxymethyl cellulose based material for sustainable/active food packaging application. J Thermoplast Compos Mater 37(6):2035–2050
12. Tohamy H-AS (2022) Reinforced modified carboxymethyl cellulose films with graphene oxide/silver nanoparticles as antimicrobial agents. Egypt J Chem 65(12):509–518
13. Tohamy H-AS (2023) Cellulosic nitrogen doped carbon quantum dots hydrogels with fluorescence/visco-elastic properties for pH-and temperature-sensitivity. Diam Relat Mater 136:110027
14. Tohamy H-AS, El-Sakhawy M, Elnasharty MM (2023) Carboxymethyl cellulose membranes blended with carbon nanotubes/ag nanoparticles for eco-friendly safer lithium-ion batteries. Diam Relat Mater 138:110205
15. Ali H, Ramadan A, Yousef M (1992) Cyanoethylation of hydroxyethyl cellulose: preparation and characterization. Polym-Plast Technol Eng 31(1–2):61–71
16. Kamel S, Hassan EM, El-Sakhawy M (2006) Preparation and application of acrylonitrile-grafted cyanoethyl cellulose for the removal of copper (II) ions. J Appl Polym Sci 100(1):329–334
17. Jia C et al (2015) Preparation and dielectric properties of cyanoethyl cellulose/$BaTiO_3$ flexible nanocomposite films. RSC Adv 5(20):15283–15291
18. Molole GJ, Gure A, Abdissa N (2022) Determination of total phenolic content and antioxidant activity of Commiphora mollis (Oliv) Engl Resin. BMC Chem 16(1):48
19. Abdallah WE, Awad HM, AbdelMohsen MM (2023) Phytochemical composition, antioxidant and antitumor activities of some date palm pollen extracts. Egypt J Chem 66(5):425–434
20. Boligon AA, Machado MM, Athayde ML (2014) Technical evaluation of antioxidant activity. Med Chem 4(7):517–522
21. Tohamy H-AS, Magar HS (2022) A flexible, low-cost, disposable non-enzymatic electrochemical sensor based on MnO_2/cellulose nanostructure. ECS J Solid State Sci Technol 11(12):127003
22. Zhou J et al (2010) A facile method for the homogeneous synthesis of cyanoethyl cellulose in NaOH/urea aqueous solutions. Polym Chem 1(10):1662–1668
23. Klančnik A et al (2010) Evaluation of diffusion and dilution methods to determine the antibacterial activity of plant extracts. J Microbiol Methods 81(2):121–126
24. McFarland J (1907) The nephelometer: an instrument for estimating the number of bacteria in suspensions used for calculating the opsonic index and for vaccines. J Am Med Assoc 49(14):1176–1178
25. Gao Z et al (1999) Free radical scavenging and antioxidant activities of flavonoids extracted from the radix of Scutellaria baicalensis Georgi. Biochimica et Biophysica Acta (BBA) Gen Subj 1472(3):643–650. https://doi.org/10.1016/S0304-4165(99)00152-X
26. Fedel-Miyasato LE et al (2014) Evaluation of anti-inflammatory, immunomodulatory, chemopreventive and wound healing potentials from *Schinus* terebinthifolius methanolic extract. Rev Bras 24:565–575
27. Tohamy H-AS (2024) Fluorescence 'turn-on'probe for chromium reduction, adsorption and detection based on cellulosic nitrogen-doped carbon quantum dots hydrogels. Gels 10(5):296
28. Ivanov M et al (2022) Polyphenols as inhibitors of antibiotic resistant bacteria—mechanisms underlying rutin interference with bacterial virulence. Pharmaceuticals 15(3):385
29. Xi M et al (2022) Potential application of luteolin as an active antibacterial composition in the development of hand sanitizer products. Molecules 27(21):7342
30. Ivanov M et al (2022) Polyphenols as inhibitors of antibiotic resistant bacteria-mechanisms underlying rutin interference with bacterial virulence. Pharmaceuticals 15:385
31. Razaviamri S, Wang K, Liu B, Lee BP (2021) Catechol-based antimicrobial polymers. Molecules 26(3):559

32. Kupnik K, Primožič M, Kokol V, Knez Ž, Leitgeb M (2023) Enzymatic, antioxidant, and antimicrobial activities of bioactive compounds from avocado (*Persea americana* L.) seed. Plants 12(5):1201
33. Biswas B et al (2013) Antimicrobial activities of leaf extracts of guava (*Psidium guajava* L.) on two gram-negative and gram-positive bacteria. Int J Microbiol 2013:746165
34. Chen C, Chang W-Y (2007) Antimicrobial activity of cotton fabric pretreated by microwave plasma and dyed with onion skin and onion pulp extractions. Indian J Fibre Text Res 32(1):122–125
35. Sadaf S et al (2023) Antimicrobial activity of comfort related properties of silk treated with herbal extracts in making of reusable masks. Biosci J 39(e39035):1981–3163
36. Wu S-C et al (2019) Natural flavones from Morus alba against methicillin-resistant *Staphylococcus aureus* via targeting the proton motive force and membrane permeability. J Agric Food Chem 67(36):10222–10234
37. Bouarab-Chibane L et al (2019) Antibacterial properties of polyphenols: characterization and QSAR (quantitative structure–activity relationship) models. Front Microbiol 10:440698
38. Liu B et al (2021) Antimicrobial property of halogenated catechols. Chem Eng J 403:126340

Publisher's Note Springer Nature remains neutral with regard to jurisdictional claims in published maps and institutional affiliations.